On Forced Temperature Changes, Internal Variability and the AMO

Michael E. Mann

Byron A. Steinman

Sonya K. Miller

Department of Meteorology and Earth and Environmental Systems Institute,

Pennsylvania State University, University Park, PA, USA 16802

Geophysical Research Letters (revised Mar 12, 2014)

Abstract

We estimate the low-frequency internal variability of Northern Hemisphere (NH) mean temperature using observed temperature variations, which include both forced and internal variability components, and several alternative model simulations of the (natural + anthropogenic) forced component alone. We then generate an ensemble of alternative historical temperature histories based on the statistics of the estimated internal variability. Using this ensemble, we show, firstly, that recent NH mean temperatures fall within the range of expected multidecadal variability. Using the synthetic temperature histories, we also show that certain procedures used in past studies to estimate internal variability, and in particular, an internal multidecadal oscillation termed the "Atlantic Multidecadal Oscillation" or "AMO", fail to isolate the true internal variability when it is *a priori* known. Such procedures yield an AMO signal with an inflated amplitude and biased phase, attributing some of the recent NH mean temperature rise to the AMO. The true AMO signal, instead, appears likely to have been in a cooling phase in recent decades, offsetting some of the anthropogenic warming. Claims of multidecadal "stadium wave" patterns of variation across multiple climate indices are also shown to likely be an artifact of this flawed procedure for isolating putative climate oscillations.

Keywords: AMO, climate oscillations, internal/forced variability, stadium waves

Index Terms: 1616, 3305, 4215

1. Introduction

Evidence for a multidecadal climate oscillation centered in the North Atlantic originated in work by Folland and colleagues during the 1980s [*Folland et al* 1984; 1986]. Additional support was provided in subsequent analyses of observational climate data [e.g. *Kushnir et al*, 1994]. The confident establishment of any low-frequency oscillatory climate signal, however, was hampered by the limited (roughly one century) length of the instrumental climate record and the potential contamination of putative low-frequency oscillations by forced long-term climate trends. Subsequent work in the mid-1990s attempted to address these limitations. *Mann and Park* [1994;1996] used a multivariate signal detection approach to separate distinct long-term climate signals, while *Schlesinger and Ramankutty* [1994] employed climate model simulations to estimate and remove the forced trend from observations. These analyses provided further evidence for a multidecadal (50-70 year) timescale signal centered in the North Atlantic with a weak projection onto hemispheric mean temperature. *Mann et al* [1995] presented evidence based on the analyses of paleoclimate proxy data that such a signal persists several centuries back in time.

Meanwhile, climate model simulations by *Delworth et al* [1993; 1997] demonstrated the existence of an internal multidecadal oscillation associated with the North Atlantic meridional overturning circulation ("AMOC") and coupled ocean-atmosphere processes in the North Atlantic. *Delworth and Mann* [2000] provided consistent evidence across instrumental observations, paleoclimate data, and coupled model simulations, for the existence of a distinct multidecadal climate mode. This mode was subsequently termed the "Atlantic Multidecadal Oscillation" ("AMO") in *Kerr* [2000]

[the term was coined by M. Mann in an interview with Kerr—see *Mann*, 2012]. In this article, we reserve the term AMO to denote such an internal, multidecadal timescale oscillation.

In most studies, the AMO surface temperature signal is found to be concentrated in the high latitudes of the North Atlantic, while the projection onto Northern Hemisphere (NH) mean temperature is modest. *Knight et al* [2005] demonstrated the existence of an AMO signal in a 1400 year control simulation of the Hadley Centre (HadCM3) coupled model with peak temperature variations approaching 0.5 ^{o}C in the high latitudes of the North Atlantic, but with an NH mean amplitude of only ~0.1^{o}C. The signal in the *tropical* North Atlantic was also found to be only ~0.1^{o}C in peak amplitude.

Some analyses have argued for a substantially larger expression of the AMO in NH mean temperature and/or tropical Atlantic temperatures [e.g. *Enfield et al*, 2001; *Goldenberg et al*, 2001; *Wyatt et al* 2012; *Wyatt and Curry*, 2013]. These studies employed what we will henceforth refer to as the "Detrended-AMO" approach: the AMO signal was defined as the low-frequency component that remains after linearly detrending surface temperatures. Other studies, however, have demonstrated likely artifacts of that procedure [*Trenberth and Shea*, 2006; *Mann and Emanuel*, 2006; *Delworth et al*, 2007; *Ting et al*, 2009]. For example, *Mann and Emanuel* [2006] show that such a procedure misattributes at least part of the forced cooling of the NH by anthropogenic aerosols during the 1950s-1970s (especially over parts of the North Atlantic) to the purported down-swing of an internal "AMO" oscillation. A number of climate modeling studies support their finding [*Santer et al*, 2006; *Booth et al*, 2012;

Evan, 2012; *Dunstone et al*, 2013], though the precise role that anthropogenic aerosols have played in recent decades continues to be debated in the literature [*Koch et al*, 2011*; Carslaw et al*, 2013; *Stevens*, 2013].

In this study, we take a different approach to diagnosing the expression of the AMO. Noting that previous studies have established that the AMO, while centered in the North Atlantic, projects onto Northern Hemisphere mean temperature, we focus specifically on its hemispheric projection. This eliminates the need for more complex spatiotemporal signal detection approaches [e.g. *Mann and Park*, 1994; *Delworth and Mann*, 2000], though it precludes drawing inferences about the regional AMO footprint. Like *Schlesinger and Ramankutty* [1994], we use model estimates of the forced trend in NH mean temperature. We account, however, for key natural (solar and volcanic) radiative forcings not included in that former study. Moreover, we use the procedure to assess the potential bias of certain approaches for detecting and defining an AMO signal. Estimating the internal variability ("AMO") component by differencing the observed and estimated forced historical NH temperature variations (henceforth the "Differenced-AMO" approach), we construct a simple statistical model for the internal variability. We then produce a set of alternative internal variability realizations and, accordingly, an ensemble of plausible synthetic NH mean temperature histories.

Using this ensemble, we firstly investigate the issue [e.g. *The Economist*, 2013; *Allen et al*, 2013] of whether temperature changes over the past decade fall within the range of expected low-frequency natural variability. Then by knowing the true "AMO" signal for each of the synthetic temperature histories, we are able to test the ability of

the Detrended-AMO approach to recover that signal. Finally, we examine the related "stadium wave" hypothesis of Wyatt and collaborators [*Wyatt et al* 2012; *Wyatt and Curry*, 2013], wherein a series of climate indices are analyzed for AMO behavior via the Detrended-AMO approach, and are interpreted as providing evidence for a coherent multidecadal oscillation propagating through the global climate system.

2. Methods

We employed a simple zero-dimensional Energy Balance Model ("EBM" —see e.g. *North et al* [1981]) of the form:

$$C\,\mathrm{d}T/\mathrm{d}t = S(1-\alpha)/4 + F_{RAD} - A - BT$$

to estimate the forced response of the Northern Hemisphere mean temperature to natural (volcanic and solar) and anthropogenic (well-mixed greenhouse gases and Northern Hemisphere mean tropospheric aerosol) radiative forcing [see *Mann* 2011; *Mann et al* 2012].

T is the temperature of Earth's surface (approximated at the surface of a 70 m depth mixed layer ocean covering 70% of Earth's surface area). C=2.08 x 10^8 J $K^{-1}m^{-2}$ is an effective heat capacity that accounts for the thermal inertia of the mixed layer ocean. $S \approx 1370$ Wm^{-2} is the "solar constant" and α=0.3 is the effective surface albedo. The linear "gray body" approximation $LW=A+BT$ was used to model outgoing long-wave radiation, where the choice of B dictates the equilibrium climate sensitivity (ECS) ΔT_{2xCO2}. For the purpose of the analyses here, we adopted a mid-range IPCC

[*Flato et al*, 2013] ECS of ΔT_{2xCO2}=3.0 ^{o}C (B=1.25 Wm^{-2}), but similar results (see Supplementary Information) are achieved for a broad range of ECS values.

F is the anthropogenic radiative forcing which includes long-wave forcing by well-mixed anthropogenic greenhouse gases as well as short-wave forcing by anthropogenic tropospheric aerosols. The latter forcing is particularly uncertain, owing to uncertainties (non-linear interactions) in indirect effects, and the difficulties of separating anthropogenic and natural aerosol forcing [see *Koch et al*, 2011; *Booth et al*, 2012; *Evan*, 2012; *Dunstone et al*, 2013; *Carslaw et al*, 2013; *Stevens*, 2013]. We thus test the sensitivity of our results to a broad range of estimated aerosol Effective Radiative Forcing ("ERF") estimates, as discussed below. Volcanic aerosol forcing and changes in solar output are represented as associated variations in S, with quantitative estimates of radiative forcing derived from geophysical evidence from ice cores and sunspot data respectively, under certain scaling assumptions. See Supplementary Information for further details.

The best fit to the observational NH series (82% variance explained) is achieved using an aerosol scaling factor of 1.2 (i.e. assuming that indirect aerosol forcing increases ERF by 20% relative to the direct forcing), linear scaling of volcanic optical depth with aerosol deposition, and a 0.25% Maunder Minimum-present solar forcing scaling assumption. These are the standard settings for the EBM experiments. Our main findings, however, are robust with respect to a range of values for these parameters. Additional experiments investigating the sensitivity of the results to the particular

forcing estimates used and aerosol scaling are provided in Supplementary Information.

The aforementioned EBM experiments have some important limitations. For example, the EBM does not account for potential changes in the flux of heat into the deep ocean, something that competes with both ECS and aerosol ERF in determining the response of surface temperatures to historical radiative forcing changes. We have thus, in addition, analyzed a comprehensive ensemble of state-of-the-art climate model simulations provided by the Coupled Model Intercomparison Project Phase 5 (CMIP5) historical simulation experiments [*Stocker et al*, 2013]. Estimates of the forced component of NH mean temperature were derived by averaging over large ensembles of independent realizations, such that the internal variability component approaches zero amplitude. We used both a sizeable ensemble (N=24) of simulations from one particular coupled model (GISS E2-R) and the even larger full CMIP5 multi-model ensemble (N=163 total realizations, M=40 models), henceforth referred to as "CMIP5-GISS" and "CMIP5-Full" respectively. The GISS-E2-R simulations all include aerosol indirect effects, and our analyses using the CMIP5-GISS ensemble thus uniformly accounts for the role of aerosol indirect effects on historical temperature trends. A logical extension of the present analysis would nonetheless involve stratifying the full CMIP5 multimodel ensemble with respect to treatment of aerosol indirect effects to more fully assess the robustness of our findings with regard to assumptions regarding aerosol indirect effects.

We estimate the unforced, internal variability through the semi-empirical Differenced-AMO approach discussed above, and introduced by *Schlesinger & Ramankutty* [1994]: We simply subtract the estimate (EBM, CMIP5-GISS, or CMIP5-Full) of the forced component from the actual observational [*Brohan et al*, 2006; updated to present] NH mean annual temperature series. We then define the "AMO" signal as the multidecadally (50 year) low-passed component of this residual series [employing the optimal smoothing method of *Mann*, 2008 (see Supplementary Information)].

We generate an ensemble of alternative internal variability realizations via a Monte Carlo approach, producing random AR(1) "red noise" realizations that preserve the amplitude and first-order autocorrelation of the empirically-estimated internal variability series described above. We use only the pre-1998 data in this procedure so that the null distribution is independent of any temperature information for the past 15 years. For each of the internal variability realizations, there is a corresponding surrogate NH mean series defined by adding the model-estimated forced component to the internal variability surrogate. The true "AMO" series for that surrogate is defined as the multidecadal low-passed component of the internal variability component alone. We also estimate the AMO component using the Detrended-AMO approach discussed earlier, wherein the NH mean series is linearly detrended, and the "AMO" is defined as the low-frequency (50 year low-pass filtered) component of the residual. Note that the use of simple red noise represents an extremely conservative null hypothesis, since the true AMO signal [e.g. *Delworth and Mann*, 2000] is argued to be a narrowband 50-70 year oscillation, rather than simple low-frequency red noise.

To investigate the supposed phenomenon of an AMO "stadium wave" among teleconnection indices, we apply the Detrended-AMO approach to a set of five synthetic climate indices constructed to each have a modest correlation with NH mean temperature (using the model NH mean temperature series). In each case, we add to the NH mean series an independent realization of Gaussian white noise with an amplitude that yields a correlation (r=0.5) with the NH mean series similar to that found empirically among Northern Hemisphere teleconnection indices [*Hurrell*, 1996]. The use of independent noise realizations reflects the null hypothesis that the various climate indices are impacted by different noise processes, and have only the underlying forced signal in common.

All raw data, ©Matlab code, and results from our analysis are available at the supplementary website:
http://www.meteo.psu.edu/~mann/supplements/GRL_AMO14

3. Results and Discussion

3.1. Modeled vs. Observed Northern Hemisphere mean temperature

In Figure 1, we compare the model (EBM, CMIP5-GISS, and CMIP5-Full) estimates of the purely forced component of Northern Hemisphere temperature from AD 1850-present. We also show an ensemble of five NH mean surrogates produced using the EBM simulation and five different noise (i.e. internal variability) realizations. The HadCRUT4 [*Brohan et al*, 2006] and GISTEMP [*Hansen et al*, 2006] instrumental

NH annual mean (land+ocean) surface temperature series through AD 2012 are shown for comparison.

It is apparent that the most recent decade is well within the ensemble spread. As we have assumed a mid-range IPCC value of equilibrium climate sensitivity in the EBM experiments, this latter observation argues against the notion that the slower rate of warming over the past decade requires [e.g. as argued in *The Economist*, 2013] any lowering of canonical ECS estimates. It is, instead, entirely consistent with the expected level of multidecadal noise. Similar results are obtained (a) in other noise ensembles, (b) varying the equilibrium climate sensitivity (ECS) over a wide range, (c) using alternative aerosol ERF estimates, (d) varying aerosol scaling, (e) using various alternative estimates of natural radiative forcing and (f) using CMIP5 model estimates (both CMIP5-GISS and CMIP5-Full) in place of the EBM estimates (Supplementary Information).

3.2. Hemispheric AMO Influence

In Figure 2 we show the estimated true historical realization of internal variability in NH mean temperature, based on the Differenced-AMO approach (differencing the observations and the model-estimated forced temperature series) using the EBM (Fig 2a), CMIP5-GISS (Fig 2b) and CMIP5-Full (Fig 2c) estimates of forced temperature change. Also shown are the multidecadally-smoothed versions of the series, which serve as estimates of the true NH mean projection of the AMO. We compare these series with the residual series obtained by a linear detrending of the NH mean temperature data followed by multidecadal smoothing, i.e. the NH mean projection of

the "AMO" series as estimated instead by the Detrended-AMO approach. The AMO oscillation in the coupled model simulations of *Knight et al* [2005] was found to have a NH mean amplitude A = 0.09 ^{o}C (standard error 0.02 ^{o}C). For a simple (i.e. sinusoidal) oscillation, the root-mean-square deviation is related to the amplitude by $\sigma = A/\sqrt{2}$. The *Knight et al* [2005] result thus gives a two standard error range σ = 0.064 +/- 0.028 ^{o}C. The AMO series estimated by the Differenced-AMO approach has a root-mean-square deviation, σ =0.054 ^{o}C (EBM), σ =0.043 ^{o}C (CMIP5 GISS E2-R), and σ =0.056 ^{o}C (CMIP5-Full), all within the uncertainty interval of the *Knight et al* estimate. By contrast, the Detrended-AMO method yields a putative AMO signal with σ =0.13 ^{o}C, twice as large as the *Knight et al* estimate, and well outside its two standard error bounds.

An additional problem with the Detrended-AMO approach (as much an issue as the *amplitude* overestimation) is the severe bias observed in the inferred *phase* of the AMO. The Detrended-AMO series using either the EBM, CMIP5-GISS or CMIP5-Full model estimate of the forced component, shows a substantial (~ -0.2 ^{o}C) negative peak in the mid 1970s and a positive peak cresting at present. As noted in previous work [*Mann and Emanuel*, 2006; *Santer et al*, 2006; *Booth et al*, 2012; *Evan*, 2012; *Dunstone et al*, 2013] the former feature is almost certainly associated with the strong anthropogenic sulphate aerosol cooling in the Northern Hemisphere from the 1950s-1970s. Applying the Detrended-AMO approach directly to the model-estimated forced component alone, we observe these same main features, including the 1950s-1970s decrease (Figure 2). We conclude that those features arise from forced changes in temperature rather than internal multidecadal variability.

The Differenced-AMO approach indeed suggests a very different AMO history, regardless of whether the EBM, CMIP-GISS or CMIP-Full series is used to estimate the forced component. Most importantly, a positive peak is now observed during the 1990s, with a subsequent decline through present (Figure 2). That decline is associated with the much-discussed [*The Economist*, 2013; *Allen et al*, 2012; *Stocker et al*, 2013] deficit of observed vs. model-predicted warming over the past decade. It is thus reasonable to infer that the real AMO has played at least a modest role in that deficit. To the extent that the AMO is an oscillatory mode, it is furthermore reasonable to assume that this cooling effect is fleeting, and that the AMO is likely to instead add to anthropogenic warming in the decades ahead.

Some recent studies indicate that initializing the state of the AMOC improves coupled model hindcasts of North Atlantic warming since the mid 1990s [*Yeager et al*, 2012; *Msadek et al*. 2013], which might appear to conflict with our finding of an AMO cooling signal during this time frame. The improvement in skill, however, may simply be a consequence of data assimilation, which serves to correct imperfect or missing model physics by "nudging" the model toward the true climate state. Given "red noise" climate persistence, such nudging guarantees that an initialized model will exhibit more near-term skill than an uninitialized model, but it doesn't tell us whether the initial state assimilated into the model was primarily a result of internal variability, forced variability, or some combination thereof.

The biasing effect of the Detrended-AMO approach becomes even clearer when we analyze the five synthetic alternative NH mean temperature realizations, and compare (Fig. 3) the true AMO signal (which is known precisely in these cases since the

internal variability was specified *a priori*) and the Detrended-AMO signal. The true AMO signals are—as they represent independent realizations of multidecadal noise—uncorrelated among the five realizations (Fig. 3a). They are seen to have random relative phase (i.e. random timings of negative and positive peaks), with typical peak amplitude A ~0.1 ^{o}C. The random surrogates are qualitatively similar in their attributes to the Differenced-AMO estimate of the real-world AMO series. By contrast, the Detrended-AMO signals (Fig. 3b) show amplitudes A ~0.25 ^{o}C that are inflated by more than a factor of two. Further, they are largely all in phase with the Detrended-AMO signal diagnosed from observations (Fig. 2), an artifact of the common forced signal masquerading as coherent low-frequency noise. The small spread in phase among the different surrogates arises from the contribution of the true random "AMO" variability shown in Fig 3a.

The above findings are robust (see Supplementary Information) with respect to whether the EBM or two different CMIP5 (GISS and Full) forced NH mean temperature estimates are used, and in the case of the EBM, the precise equilibrium climate sensitivity, particular anthropogenic aerosol forcing series used, and assumptions regarding the amplitude of indirect aerosol forcing.

3.3. "Stadium Waves"

Finally, we examine the simulation of five AMO-related "indices". Each index, as noted earlier, has been degraded with an independent realization of additive white noise to have a correlation of r=0.5 with the modeled NH mean temperature series, and then smoothed to highlight multidecadal (greater than 50 year) timescale

variability. The multidecadal noise component is once again random and uncorrelated across series by construction (Fig. 4a), so any "oscillation" that is coherent across the five series must come instead from the common forced component. Indeed, the Detrended-AMO approach (Fig. 4b) yields an apparent multidecadal "AMO" oscillation that is coherent across the indices, an artifact of the residual forced signal masquerading as an apparent low-frequency oscillation. The apparent "AMO" signal is most coherent across indices during the most recent half century, when the forcing is largest.

Another important feature apparent in this comparison is that the low-frequency noise leads to substantial perturbations in the overall "phase" of the apparent "AMO" signal (Fig. 4b) giving the appearance of a propagating wave or "stadium wave" in the parlance of *Wyatt et al* [2012]. In previous work applying the Detrended-AMO approach to estimate the "AMO" signal in a wide variety of climate indices [*Wyatt et al*, 2012; *Wyatt and Curry*, 2013], such a feature was interpreted as an indication of an AMO oscillation impacting a wide range of climate phenomena as it propagates through the climate system. Our analysis suggests that this feature is instead an artifact of the residual forced signal that remains after linear detrending (the Detrended-AMO procedure), combined with random perturbations in the apparent phase of the "oscillation" for any particular climate index, due to the low-frequency effects of the additive noise.

Although the precise results depend (see Supplementary Information) on the particular estimate (EBM, CMIP5-GISS or CMIP5-Full) used for the forced signal, and in the case of the EBM, the assumed equilibrium climate sensitivity, as well as

the forcing series used and the amplitude of indirect effects assumed, the basic conclusions above are once again robust with respect to all such details.

4. Conclusions

By comparing model-based estimates of forced temperature changes (using both an EBM and ensemble means of the CMIP5 model simulations) with observed NH mean temperatures over the historical era, we are able to empirically diagnose the internal variability component of NH mean temperature. A simple statistical model applied to that component is then used to generate an ensemble of noise realizations and an ensemble of alternative NH mean temperature series. Actual NH mean temperatures—including the temperature trend over the past decade—are shown to be consistent with that ensemble. We conclude that there is no inconsistency between recent observed and modeled temperature trends. As a corollary, recent temperature observations are entirely consistent with prevailing mid-range estimates of climate sensitivity.

We use the same ensemble to evaluate the faithfulness of the "Detrended Residual" approach to estimating internal (AMO-related) variability, wherein temperature data are linearly detrended, the residual is interpreted as internal variability, and the multidecadal component of the residual is interpreted as representing a low-frequency "AMO" oscillation. In cases where the signal is known *a priori*, we show that this procedure yields a biased estimate of the true AMO signal in the data. The procedure attributes too large an amplitude to the AMO signal and a biased estimate of its phase. Wherein application of the flawed Detrended-AMO approach attributes some of the

recent NH mean temperature rise to an AMO signal, the true AMO signal instead appears likely to have contributed to a relative *cooling* over the past decade, explaining some of the observed slowing of warming during that timeframe. We find that claims of a "stadium wave" AMO signal propagating through the global climate are likely an artifact of the Detrended-AMO procedure as well.

Acknowledgements:

All raw data, ©Matlab code, and results from our analysis are available at the supplementary website: http://www.meteo.psu.edu/~mann/supplements/GRL_AMO14. We thank Drew Shindell, Ron Miller, Larisa Nazarenko and Gavin Schmidt of NASA/GISS for input regarding aerosol forcing estimates and provision of the GISS NINT aerosol forcing series. BAS acknowledges the U.S. National Science Foundation AGS-PRF (AGS-1137750). We also thank the two anonymous reviewers of the manuscript for their helpful comments.

References

Allen, M. R., J. F. B. Mitchell, and P. A. Stott (2013), Test of A Decadal Climate Forecast, *Nat. Geosci.*, *6*, 243–244.

Booth, B. B. B., N. J. Dunstone, P. R. Halloran, T. Andrews, and N. Bellouin (2012), Aerosols implicated as a prime driver of twentieth-century North Atlantic climate variability, *Nature*, *484*, 228–232.

Boucher et al. (2013) Clouds and Aerosols. In Climate change 2013: the physical science basis. Working Group I contribution to the Fifth Assessment Report of the Intergovernmental Panel on Climate Change (eds. Stocker et al.).

Brohan, P., J. J. Kennedy, I. Haris, S. F. B. Tett, and P. D. Jones (2006), Uncertainty estimates in regional and global observed temperature changes: a new dataset from 1850, *J. Geophys. Res.*, *111*, D12106, doi:10.1029/2005JD006548.

Carslaw et al. (2013), Large contribution of natural aerosols to uncertainty in indirect forcing, *Nature*, 503, 67-71.

Delworth, T., S. Manabe, and R. J. Stouffer (1993), Interdecadal variations of the thermohaline circulation in a coupled ocean-atmosphere model, *J. Clim.*, *6*, 1993–2011.

Delworth, T. L., S. Manabe, and R. J. Stouffer (1997), Multidecadal climate variability in the Greenland Sea and surrounding regions: A coupled model simulation, *Geophys. Res. Lett.*, *24*, 257–260.

Delworth, T. L., and M. E. Mann (2000), Observed and Simulated Multidecadal Variability in the Northern Hemisphere, *Clim. Dynam.*, *16*, 661–676.

Delworth, T. L., R. Zhang, and M. E. Mann (2007), Decadal to Centennial Variability of the Atlantic from Observations and Models, in Past and Future Changes of the Oceans Meridional Overturning Circulation: Mechanisms and Impacts, Geophys.

Monogr. Ser., vol. 173, edited by A. Schmittner, J. C. H. Chiang, and S. R. Hemming, pp.131–148, AGU, Washington, D. C.

Dunstone N. J, D. M. Smith, B. B. B. Booth, L. Hermanson, and R. Eade (2013), Anthropogenic aerosol forcing of Atlantic tropical storms, *Nat. Geosci.*, *6*, 534–539, doi:10.1038/NGEO1854.

Enfield, D. B., A. M. Mestas-Nuñez, and P. J. Trimble (2001), The Atlantic multidecadal oscillation and its relation to rainfall and river flows in the continental US, *Geophys. Res. Lett*., *28*, 2077–2080.

Evan, A. (2012), Aerosols and Atlantic aberrations, *Nature*, *484*, 170–171. doi:10.1038/nature11037, 2012.

Flato et al. (2013) Evaluation of Climate Models. In Climate change 2013: the physical science basis. Working Group I contribution to the Fifth Assessment Report of the Intergovernmental Panel on Climate Change (eds. Stocker et al.).

Folland, C. K., D. E. Parker, and F. E. Kates (1984), Worldwide marine temperature fluctuations 1856-1981, *Nature*, *310*, 670–673.

Folland, C. K., D. E. Parker, and T. N. Palmer (1986), Sahel rainfall and worldwide sea temperatures 1901–85, *Nature*, *320*, 602–607.

Goldenberg, S. B., C. W. Landsea, A. M. Mestas-Nuñez, and W. M. Gray (2001), The recent increase in Atlantic hurricane activity: Causes and implications, *Science*, *293*, 474–479.

Hansen, J., Mki. Sato, R. Ruedy, K. Lo, D.W. Lea, and M. Medina-Elizade, 2006: Global temperature change. *Proc. Natl. Acad. Sci.*, **103**, 14288-14293, doi:10.1073/pnas.0606291103.

Hurrell, J. W. (1996), Influence of Variations in Extratropical Wintertime Teleconnections on Northern Hemisphere Temperature, *Geophys. Res. Lett*., *23*, 665–668.

Kerr, R. A. (2000), A North Atlantic climate pacemaker for the centuries, *Science*, *288*, 1984–1985.

Knight, J. R., R. J. Allan, C. K. Folland, M. Vellinga, and M. E. Mann (2005), A Signature of Persistent Natural Thermohaline Circulation Cycles in Observed Climate, *Geophys. Res. Lett*., *32*, L20708, doi: 10.1029/2005GL02423.

Koch, D. et al. (2011), Coupled aerosol-chemistry-climate twentieth century transient model investigation: Trends in short-lived species and climate responses. *J. Climate*, *24*, 2693–2714, doi:10.1175/2011JCLI3582.

Kushnir, Y. (1994), Interdecadal variations in North Atlantic sea surface temperature and associated atmospheric conditions, *J. Clim.*, *7*, 141–157.

Mann, M. E. (2008), Smoothing of Climate Time Series Revisited, *Geophys. Res. Lett*., *35*, L16708, doi:10.1029/2008GL034716.

Mann, M. E. (2011), On Long Range Dependence in Global Surface Temperature Series, *Climatic Change*, *107*, 267–276.

Mann, M. E. (2012), The Hockey Stick and the Climate Wars, Columbia University Press, New York, N. Y., pp. 384.

Mann, M. E., and J. Park (1994), Global-scale modes of surface temperature variability on interannual to century timescales, *J. Geophys. Res.*, *99*, 819–833.

Mann, M. E., J. Park, and R. S. Bradley (1995), Global interdecadal and century-scale climate oscillations during the past 5 centuries, *Nature*, *378*, 266–270.

Mann, M. E., and J. Park (1996), Joint Spatio-Temporal Modes of Surface Temperature and Sea Level Pressure Variability in the Northern Hemisphere During the Last Century, *J. Clim.*, *9*, 2137–2162.

Mann, M. E., and K. A. Emanuel (2006), Atlantic Hurricane Trends linked to Climate Change, *Eos*, *87*(24), 233–241.

Mann, M. E., J. D. Fuentes, and S. Rutherford (2012), Underestimation of Volcanic Cooling in Tree-Ring Based Reconstructions of Hemispheric Temperatures, *Nat. Geosci.*, *5*, 202–205.

Msadek, R., W. E. Johns, S. G. Yeager, G. Danabasoglu, T. L. Delworth, and A. Rosati, (2013),,The Atlantic meridional heat transport at 26.5ºN and its relationship with the MOC in the RAPID array and the GFDL and NCAR coupled models *J. Climate*, *26*, 4335–4356.

North, G. R., R. F. Cahalan, and J. A. Coakley (1981), Energy balance climate models, *Rev. Geophys.*, *19*, 91–121.

Santer, B. D., T. M. L. Wigley, P. J. Gleckler, C. Bonfils, M. F. Wehner, K. AchutaRao, T. P. Barnett, J. S. Boyle, W. Brüggemann, M. Fiorino, N. Gillett, J. E. Hansen, P. D. Jones, S. A. Klein, G. A. Meehl, S. C. B. Raper, R. W. Reynolds, K. E. Taylor, and W. M. Washington (2006), Forced and unforced ocean temperature changes in Atlantic and Pacific tropical cyclogenesis regions, *Proc. Natl. Acad. Sci. USA*, *103*, 905–910.

Schlesinger, M. E., and N. Ramankutty (1994), An oscillation in the global climate system of period 65– 70 years, *Nature*, *367*, 723–726.

Stevens, B. (2013), Aerosols: Uncertain then, irrelevant now, *Nature*, *503*, 47–48.

Stocker et al. (2013) Climate Change 2013: The Physical Science Basis - Summary for Policymakers. In Climate change 2013: the physical science basis. Working Group I contribution to the Fifth Assessment Report of the Intergovernmental Panel on Climate Change (eds. Stocker et al.).

Ting, M., Y. Kushnir, R. Seager, and C. Li (2009), Forced and internal twentieth-century SST trends in the North Atlantic, *J. Clim.*, *22*, 1469–1481.

Trenberth, K. E., and D. J. Shea (2006), Atlantic hurricanes and natural variability in 2005, *Geophys. Res. Lett.*, *33*, L12704, doi:10.1029/2006GL026894.

The Economist (editorial), "A Sensitive Matter", March 30, 2013. http://www.economist.com/news/science-and-technology/21574461-climate-may-be-heating-up-less-response-greenhouse-gas-emissions

Wyatt, M. G., S. Kravtsov, and A. A. Tsonis (2012), Atlantic multidecadal Oscillation and Northern Hemisphere's climate variability, *Clim. Dynam.*, *38*(5–6), 929–949. doi:10.1007/s00382-011-1071-8.

Wyatt, M. G., and J. A. Curry (2013), Role for Eurasian Arctic shelf sea ice in a secularly varying hemispheric climate signal during the 20th century, *Clim. Dynam.*, doi: 10.1007/s00382-013-1950-2.

Yeager, S., A. Karspeck, G. Danabasoglu, J. Tribbia, and H. Teng (2012), A Decadal Prediction Case Study: Late Twentieth-Century North Atlantic Ocean Heat Content. *J. Climate*, *25*, 5173–5189.

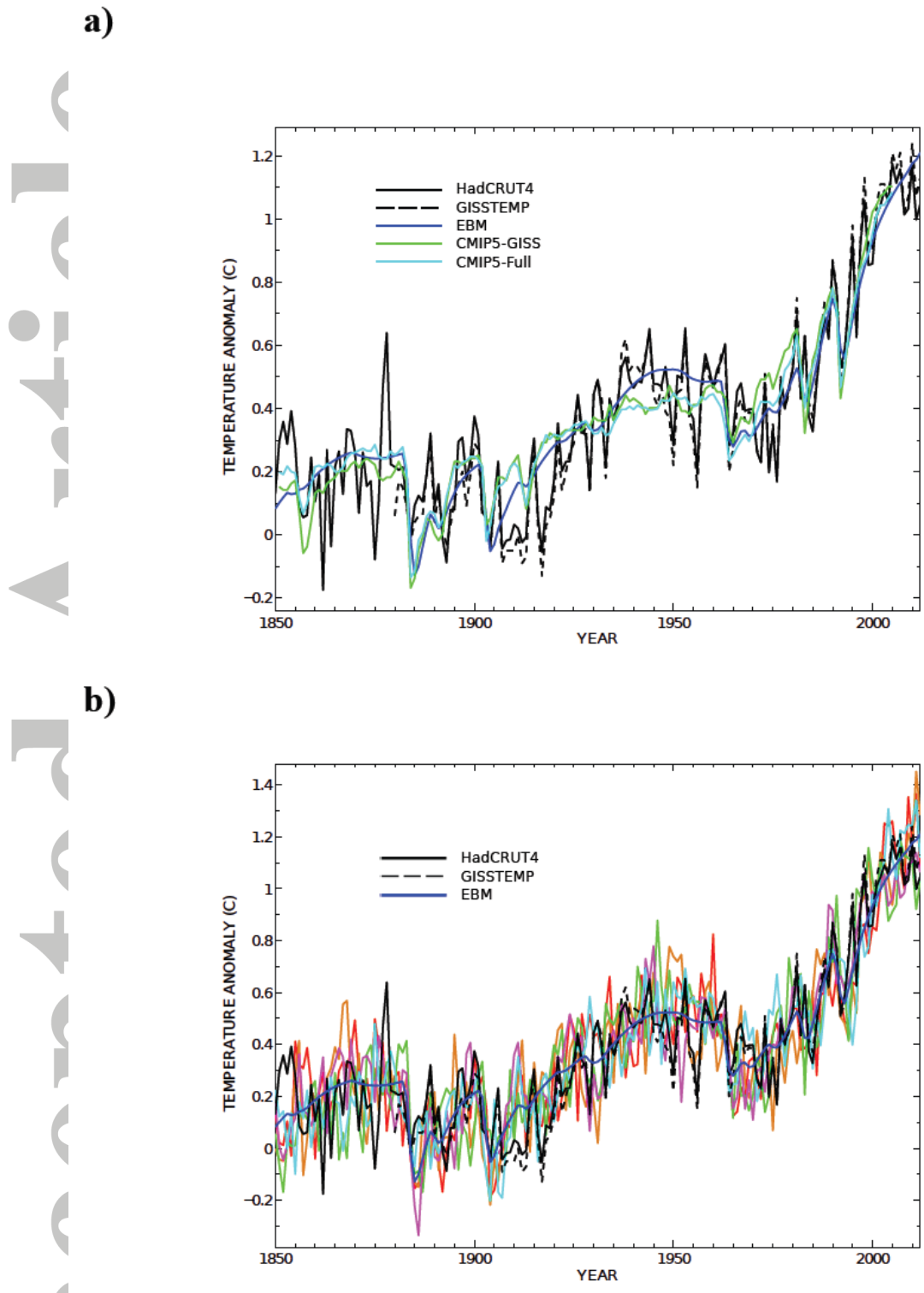

Figure 1. Simulated vs. Observed NH mean temperatures. (a) Instrumental annual [HadCRUT4—solid black, GISTEMP—dashed black) NH mean temperatures (AD 1850-2012) along with model-based estimates of forced component using EBM (blue), CMIP5-GISS (green) and CMIP5-Full (cyan). Also shown (b) are EBM-simulated series (blue) along with an ensemble of five different realizations (red, orange, blue, green, cyan) of the estimated internal variability contribution [see Supplementary Information for corresponding results based on CMIP5 simulations]. Anomalies are relative to a pre-industrial (AD 1750-1850) reference period mean.

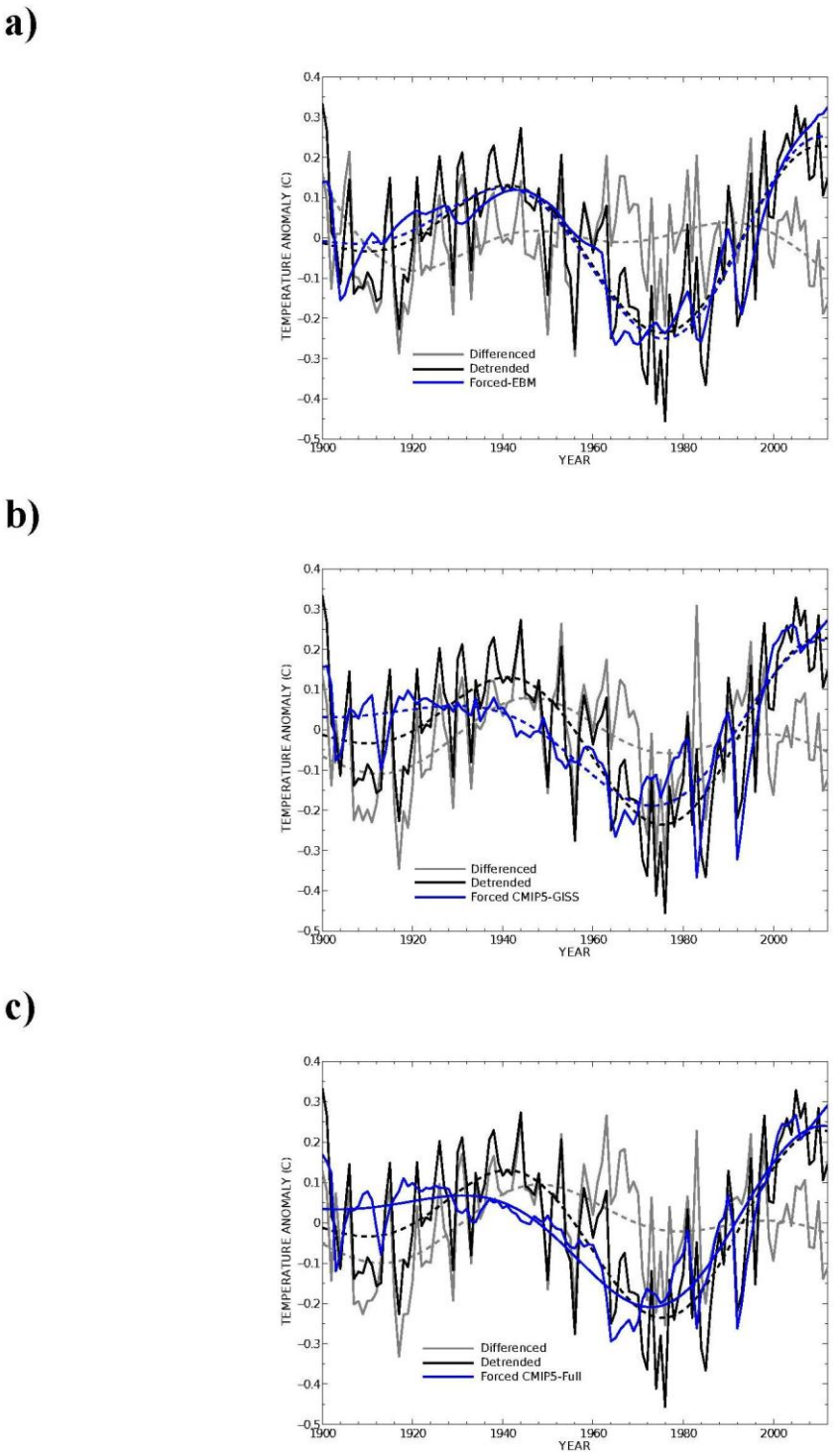

Figure 2. Time series of estimated unforced NH mean variability (annual series) and associated multidecadal "AMO" components (smooth curves) based on Differenced-AMO (gray) vs. Detrended-AMO (black) approaches applied to the observational NH mean record, using (a) EBM simulation, (b) CMIP5-GISS and (c) CMIP5-Full. Shown for comparison (blue) is the Detrended-AMO approach applied to the model-simulated forced series alone. For CMIP5 cases (i.e. b. and c.) the model series end in 2005 but have been extended to 2012 by persistence of the 30 year trend. Similar results are obtained based on persistence of the 2005 value [see Supplementary Information].

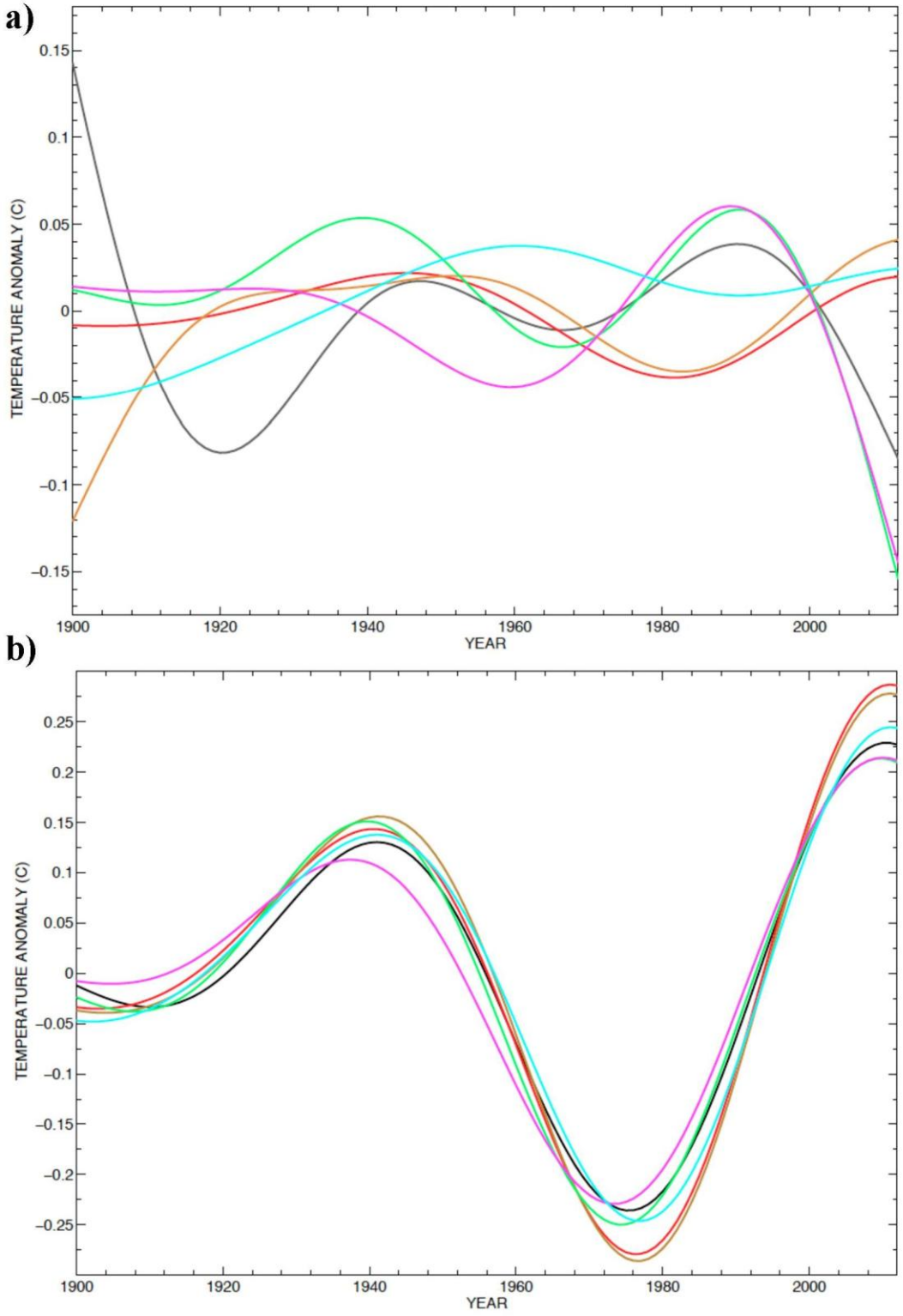

Figure 3. Comparison of (a) true NH mean AMO signal (as *a priori* defined) and (b) NH mean AMO signal as estimated by the Detrended-AMO procedure, applied to EBM simulations. Colors correspond to the same five noise realizations shown in Fig. 1. (a) The empirically-estimated Differenced-AMO signal estimate of Fig. 2 (gray). (b) The empirically-estimated Detrended-AMO signal estimate of Fig. 2 (black). See Supplementary Information for corresponding results using CMIP5 simulations.

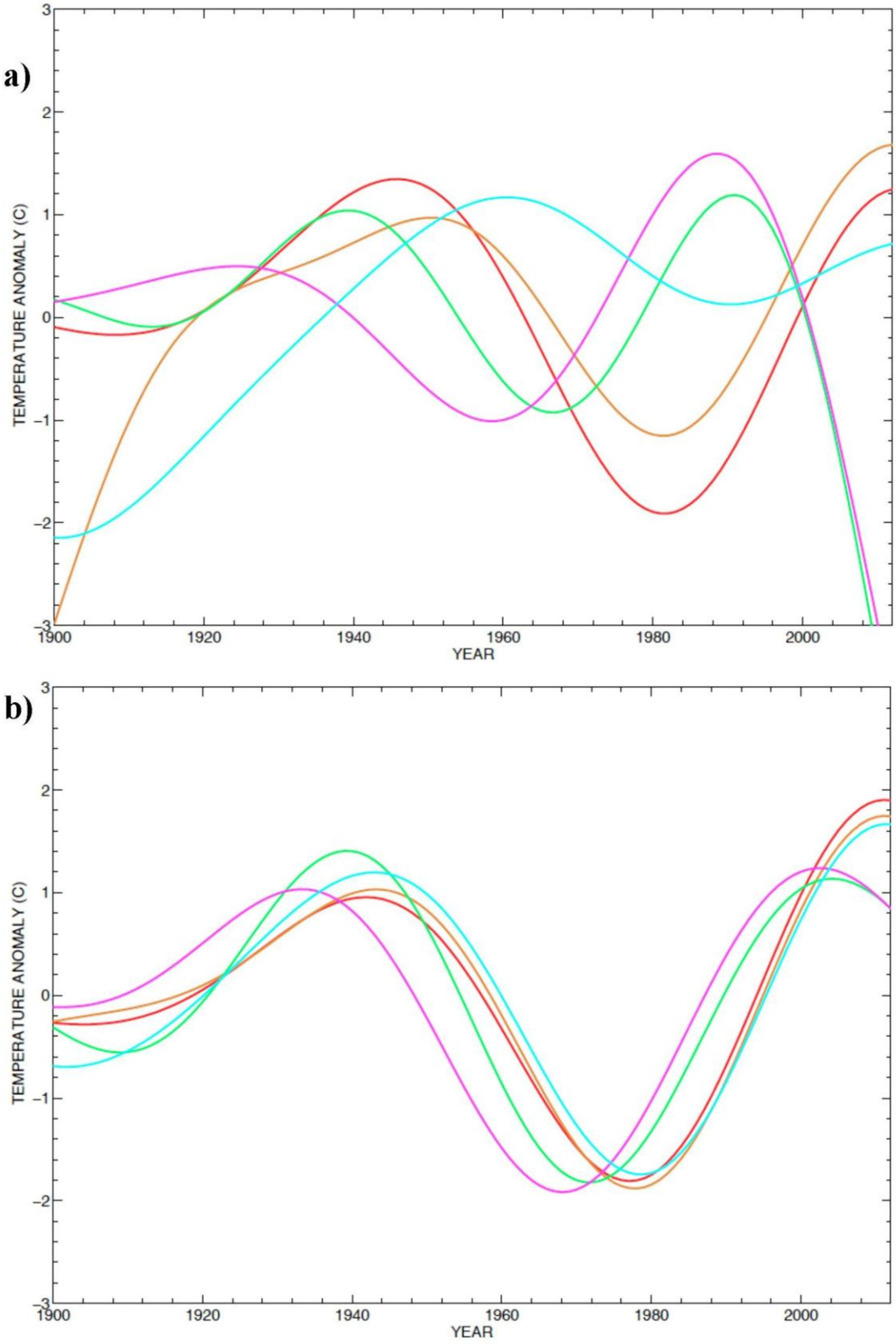

Figure 4. Comparison of (a) true AMO signal (as *a priori* defined) and (b) AMO signal as estimated by Detrended-AMO procedure, for the five synthetic standardized climate indices as described in text, using the EBM simulation. Series are standardized to have unit variance. See Supplementary Information for corresponding results using CMIP5 simulations.